Programmable Materials

International Edition: DOI: 10.1002/anie.201505013
German Edition: DOI: 10.1002/ange.201505013

Biocatalytic Feedback-Driven Temporal Programming of Self-Regulating Peptide Hydrogels

*Thomas Heuser, Elisabeth Weyandt, and Andreas Walther**

Abstract: *Switchable self-assemblies respond to external stimuli with a transition between near-equilibrium states. Although being a key to present-day advanced materials, these systems respond rather passively, and do not display autonomous dynamics. For autonomous behavior, approaches must be found to orchestrate the time domain of self-assemblies, which would lead to new generations of dynamic and self-regulating materials. Herein, we demonstrate catalytic control of the time domain of pH-responsive peptide hydrogelators in a closed system. We program transient acidic pH states by combining a fast acidic activator with the slow, enzymatic, feedback-driven generation of a base (dormant deactivator). This transient state can be programmed over orders of magnitude in time. It is coupled to dipeptides to create autonomously self-regulating, dynamic gels with programmed lifetimes, which are used for fluidic guidance, burst release, and self-erasing rapid prototyping.*

Stimuli-responsiveness in self-assemblies and materials is one of the cornerstones of soft-matter research, as it enables fundamental investigations of structure formation[1] and the targeting of switchable materials with advanced functionalities, as needed in photonics,[2] for hydrogels,[4] actuation (bilayers),[5] and controlled release.[6] Such switchability relies on the responsiveness of self-assemblies to external signals, such as temperature, the pH value, or light, and is well-understood for a range of systems.[7] On a conceptual level, such property changes are rather passive in nature: Classical stimuli-responsive systems always need an outside trigger to induce a one-way transition between thermodynamically stable states (e.g. assembly/disassembly). The resulting state will be infinitely stable, and a counter-trigger is needed to revert the system (see Figure S1). The simultaneous addition of a trigger and a counter-trigger (e.g. H^+/OH^-) typically leads to their instantaneous annihilation. Hence, autonomous behavior in the time domain and self-regulating behavior is not found. In stark contrast, natural non-equilibrium systems,[8] which are orchestrated by kinetically and catalytically controlled conversions, feedback mechanisms, and constant energy dissipation, display orchestrated dynamics in the time domain. They present prominent examples of self-regulation and adaptive behavior in general, thus offering inspiration for new concepts in the design of dynamic materials.

Hydrogels formed by self-assembly or cross-linking are vital for a range of technologies, for example, in food, materials, bio-, and life sciences, and serve as model materials for the study of fundamental approaches to structure matter.[9] Despite intense development, it has remained a challenge to advance their properties from classical, passive responsiveness to create systems that show autonomous dynamics and self-regulation. Most prominent is the coupling of tailored hydrogels to the serendipitously discovered Belousov–Zhabotinsky reaction to generate pulsating hydrogels useful for pumping or transport.[10] More recent oscillators target rational design by defined chemical or enzymatic reaction networks.[11] Routes toward single transient states in closed systems include kinetically controlled transformations of peptide nanofibril precursors[12] or dissipative structure formation.[13]

We recently showed that transient states can be programmed in time by playing a different kinetic trick.[14] We demonstrated autonomously self-regulating, transient pH states in alkaline media through the simultaneous injection of fast promoters and slow, dormant deactivators (DDs). Such transient pH jumps can be coupled to virtually all self-assembling systems operating in the targeted pH regime, whereupon they form and decay on a preprogrammed course in closed systems as encoded by the pH profile. The main advantage is that such rationally programmed pH states open a facile and generic pathway to impart artificial self-regulation and programmed lifetimes to diverse switchable self-assemblies.

Herein we provide a new approach and demonstrate catalytic and feedback-driven control over a transient, self-regulating pH state in the acidic regime, and use it in conjunction with the self-assembly of dipeptide gelators. We achieve programmable time signatures and reveal progress from an earlier self-assembly level[14] to a materials level, by now showing full gelation and hydrogel lifetimes that can be programmed with very high confidence across orders of magnitude in time in closed systems. We also identify first applications of such time-programmed self-regulating hydrogels by developing injectable solutions for temporal blocking and fluidic guidance within fluidic systems, for burst-release systems, and for self-erasing micromolded gels.

We focus on transient states in the acidic pH regime, as obtained by the kinetic balance of a fast promoter (acidic buffer) and a dormant deactivator, which are added simultaneously (Figure 1a; see also Figure S1 in the Supporting Information). The active deactivator (base) is generated in a highly time controlled manner by the urease-catalyzed

[*] T. Heuser, E. Weyandt, Dr. A. Walther
DWI—Leibniz Institute for Interactive Materials
Forckenbeckstrasse 50, 52056 Aachen (Germany)
E-mail: walther@dwi.rwth-aachen.de
Homepage: http://www.dwi.rwth-aachen.de

Supporting information for this article is available on the WWW under http://dx.doi.org/10.1002/anie.201505013.

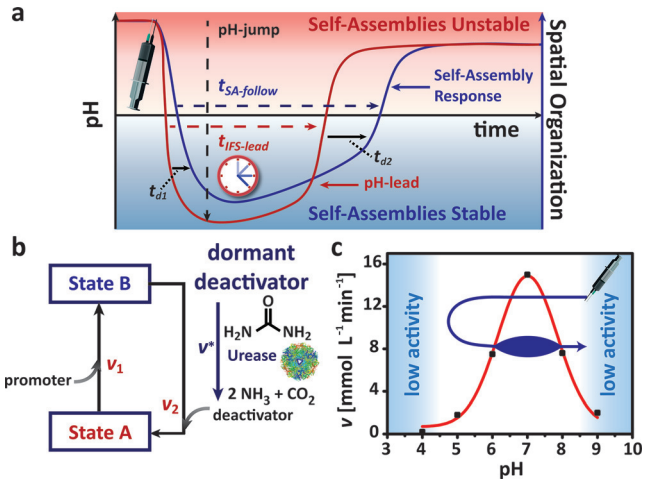

Figure 1. Enzymatic, feedback-controlled programming of transient pH profiles for the temporal programming of self-assemblies. a) The simultaneous injection of a promoter and a DD programs a transient acidic pH profile (red line, $t_{IFS\text{-}lead}$). The self-assembly follows (blue line, $t_{SA\text{-}follow}$) with kinetic offsets, t_{d1} and t_{d2}. b) Temporal programming of pH-switchable self-assemblies by controlling the availability of the deactivator. The kinetic balance of the promoting and deactivating reaction is $v_1 \gg v^*$; $v_1 \approx v_2$ becomes irrelevant. Ultimately, the excess of DD leads to recovery of the pH value. c) Bell-shaped pH-dependent urease activity with the hypothetical jump indicated.[3]

conversion of urea into CO_2 and NH_3 (Figure 1b). This rate (v^*) can be controlled by the biocatalyst concentration and is highly pH dependent (Figure 1c).[15] Base generation provides negative pH feedback and lifts the pH value back up without any external interference (closed system). Urease was used earlier to control homogeneous base generation,[16] and continuous addition with an acid in open stirred reactors allowed the production of oscillations.[17] However, we are not targeting linear pH changes or oscillations, but precisely programmed, nonlinear transient states. Such an approach has not been described previously and involves further considerations. More importantly, we couple these states with a switchable dipeptide gelator to program hydrogel lifetimes. We term the overall system an internal feedback system (IFS), in which "internal" clearly expresses that outside triggers are not needed. This transient acidic state goes conceptually beyond complementing our earlier transient alkaline state,[14] for which we relied on the constant hydrolysis of an unstable compound to provide the active deactivator. The first major advantage of the present approach is the catalytic nature of the process, which provides a unique way to fine-tune the speed of base generation through the enzyme concentration.[18] Second, the bell-shaped curve of the enzymatic activity is interesting, as it provides low enzyme activity at high and low pH values (pH < 3.5 or pH > 9; Figure 1c). Hence, the system is forcefully activated from the nearly inactive alkaline state (pH > 9) into the activity window (pH > 3.5) upon injection of the promoter. The bell-shaped activity curve leads to beneficial steep pH recovery, as the activity is self-enforcing (positive feedback) when the enzyme passes from an area of low activity at low pH values to high activity at intermediate pH values. Finally, the rate is also self-diminishing in terms of the pH value, as base generation pushes the enzyme out of its active window.

We first focus on programming the timescale, $t_{IFS\text{-}lead}$, and the pH jump of the transient acidic pH profile. The depth of the pH jump is limited by the properties of the urease (from *Canavalia ensiformis*) to a level at which the enzyme still shows sufficient activity to enable pH feedback. Therefore, we injected urease (15000–50000 catalytic units per gram; 0.1 g L^{-1}) into urea solutions (20 mM) with different starting pH values as adjusted by HCl (Figure 2a). Three different regimes can be observed: I) Above a pH_{start} value of 3.5,

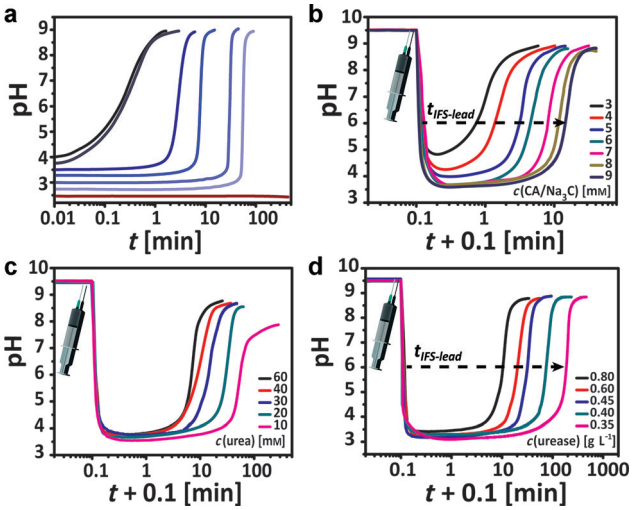

Figure 2. Programming of transient acidic pH states. a) The pH_{start} value controls the enzyme activity and the rate of base generation (20 mM urea, 0.1 g L^{-1} urease). b) The concentration of the CA/Na_3C buffer regulates the timescale (60 mM urea, 0.3 g L^{-1} urease, and various concentrations of the CA/Na_3C (4:1) buffer as a promoter. c) Influence of the substrate concentration on the timescale (0.3 g L^{-1} urease, 7 mM CA/Na_3C (4:1) buffer, and various urea concentrations). d) Catalytic control of the timescale by changing the urease concentration (60 mM urea, 12 mM CA/Na_3C (9:1) buffer).

a steep increase to a plateau at approximately pH 9 occurs (gray curves); II) in the range of pH_{start} 2.5–3.5, an increase still occurs; however, it begins with an increasingly elongating plateau for lower pH_{start} values, followed by an abrupt and steep transition; III) no increase occurs for $pH_{start} < 2.5$, thus indicating that the enzyme is inactive. The plateau at low pH values in the intermediate regime (II) is caused by the initially low catalytic activity of the urease and slow base generation. At $pH_{start} > 3.5$, the enzyme is directly in the pH window of high catalytic activity, and the increase occurs immediately . All curves level off at the same alkaline pH value, because the enzyme leaves its active zone and an ammonia buffer forms around pH 9. Therefore, the depth of the pH jump is limited to pH > 2.5 to allow for a return, and the depth of the pH jump needs to be very precise to enable reliable programming of the transient state.

Next, we establish the full IFS by a single injection of a urea-containing acidic buffer solution (promoter + DD) into basic urease solutions at pH_{start} 9.5, which is in the

alkaline low-activity area of urease. We choose acidic buffers over pure acid as rapid promoters because they enable 1) a jump to a certain pH level with high confidence, and 2) the extension of $t_{IFS\text{-}lead}$ by increasing the buffer capacity. Specifically, we selected a citric acid/sodium citrate buffer (CA/Na_3C), because preliminary investigations revealed superior homogeneity of the targeted dipeptide hydrogels as compared to those formed in phosphate buffers (possibly a counterion effect).

CA/Na_3C buffers can be adjusted over a wide pH value and ionic strength range by the combination of different ratios of CA/Na_3C and different total concentrations. Figure 2b depicts the influence of the buffer concentration (CA/Na_3C 4:1) on the IFS (60 mmol urea, 0.3 $g\,L^{-1}$ urease). Several phenomena are observed. First, as expected, increasingly deeper pH jumps occur as the buffer capacity is increased (see Figure S2 for the quantification and discussion of this behavior for different CA/Na_3C mixtures). More importantly, the transient plateaus at low pH values indeed extend upon the injection of buffers with higher capacity, because the buffers scavenge the generated base. Since all curves are in regime I of the enzymatic activity (pH jump > 3.5; high activity), the elongation of the plateau time can mainly be attributed to the increasing buffer capacity. This result demonstrates that the use of buffers is one key to the extension of $t_{IFS\text{-}lead}$. We further study the influence of the substrate concentration (DD, urea; Figure 2c) under otherwise constant conditions and find elongating plateaus for lower substrate concentrations. This result reflects the Michaelis–Menten kinetics, which rationalizes an asymptotical increase of the reaction rate with substrate concentration. The Michaelis–Menten constant of the urease is in the range of 2.9–3.6 mM.[3,19] Interestingly, low urea concentrations (10 mM) limit the pH-value rise owing to the small amount of base-generating substrate. To exclude any ambiguities, we keep the substrate concentration constant at 60 mM.

The crucial advantage of a biocatalytic pH-IFS is that the generation of the active deactivator is coupled to the maximum turnover number (TON) of the enzyme. Hence, the enzyme concentration ultimately governs the rate and provides the most precise means to fine-tune the reaction rate. Furthermore, variation of the urease concentration under otherwise constant conditions minimizes any adverse effects of the pH-dependent activity induced by jumps with different buffer concentrations (Figure 2a,b; see also Figure S2). Figure 2d clearly shows that $t_{IFS\text{-}lead}$ can be tuned with high confidence from 10 to 190 min by changing the enzyme concentration from 0.35 to 0.80 $g\,L^{-1}$ (at pH 6).

In summary, the careful screening of the reaction conditions establishes how the amount of activator (buffer), the depth of the pH jump, and most importantly, the enzyme concentration can be used to program the timescale of the transient non-equilibrium pH profile. The accessible timescales range from several minutes to hours. Further tuning to days appears feasible by increasing the buffer capacity and lowering the urease concentration. Multiple jumps are possible upon reinjection of the activator when an excess of DD is added at the beginning of the reaction (see Figure S3).

To approach the time-programmed generation of self-assemblies and hydrogels, we couple our IFS to a carefully selected dipeptide, Fmoc-Leu-Gly-OH,[20] which forms well-defined, self-assembled, twisted ribbon-type nanofibrils and hydrogels at low pH values as a result of the removal of electrostatic repulsion (Figure 3a,c). The transition to a nanofibrillar gel state occurs at approximately pH 5.8 and a peptide concentration of about 0.6 wt%. The dipeptide changes the pH evolution of the system as a result of coupling with the IFS (Figure 3b). The pH-jump depth and the plateau are coupled to the peptide concentration and its respective pK_a value. Both effects are due to the dipeptide carboxylate groups, which consume protons of the promoting CA/Na_3C buffer during the first jump, thus causing self-assembly into nanofibrils (sol→gel). Later on, they contribute to the buffer capacity and delay the return to a high pH value, thereby also delaying the disassembly (gel→sol; see Figure S4 for concentration-dependent titration curves). Macroscopically, upon injection of the IFS, the aqueous dipeptide solutions rapidly form self-supporting hydrogels, which then revert back to the sol state as programmed by the IFS and confirmed by the rheology (see Figure S5). The associated transient gel times, t_{gel}, were quantified by simple tube-inversion tests (Figure 3d,e) to range from 20 min to 11 h, as programmed by changing the urease concentration from 1 to 0.45 $g\,L^{-1}$. There are only small differences between the degelation (gel→sol; t_{gel}) and the programmed timescale of the IFS ($t_{IFS\text{-}lead}$), thus indicating only small kinetic offsets during disassembly (t_{d2}, Figure 1a).

Next, we demonstrate first applications of the time-programmed dynamic hydrogels in fluidic systems, for burst release, and for transient rapid prototyping. In both technical and biological fluidic networks (e.g. blood vessels) the time-programmed regulation of fluidic pathways may be desirable to enable the guidance or time-programmed blocking of liquids and reactants. Fields of application could be diverse, from reaction engineering to separation, fluid logics,[21] or the clamp-free blocking of blood flow during catastrophic injury. To this end, we first developed an injectable variant of the time-programmed hydrogel by using double-barreled syringes with the peptide and urease in compartment A and an acidic solution of urea in compartment B. Upon extrusion through a micromixing needle, these two compartments mix and gelation occurs as a result of a decrease in the pH value. The simultaneous mixing of urea and urease then in turn slowly returns the medium to an alkaline state and redissolves the formed gel. For better visualization, we added a pH-tracer dye (resazurin).

To demonstrate the applicability of our system to fluidic guidance, we designed a poly(dimethylsiloxane) device with a short dominant fluid channel and an alternative bypass, which is unfavorable for the fluid stream owing to a significant pressure difference (Figure 4a; see also Movie S1 in the Supporting Information). Sealing of the dominant fluid channel with a time-programmed hydrogel plug forces the fluid stream along the bypass for as long as programmed by the IFS, before it is redirected to the original path as a result of dissolution of the time-programmed hydrogel by the use of its internal trigger. Operations and repair could be performed

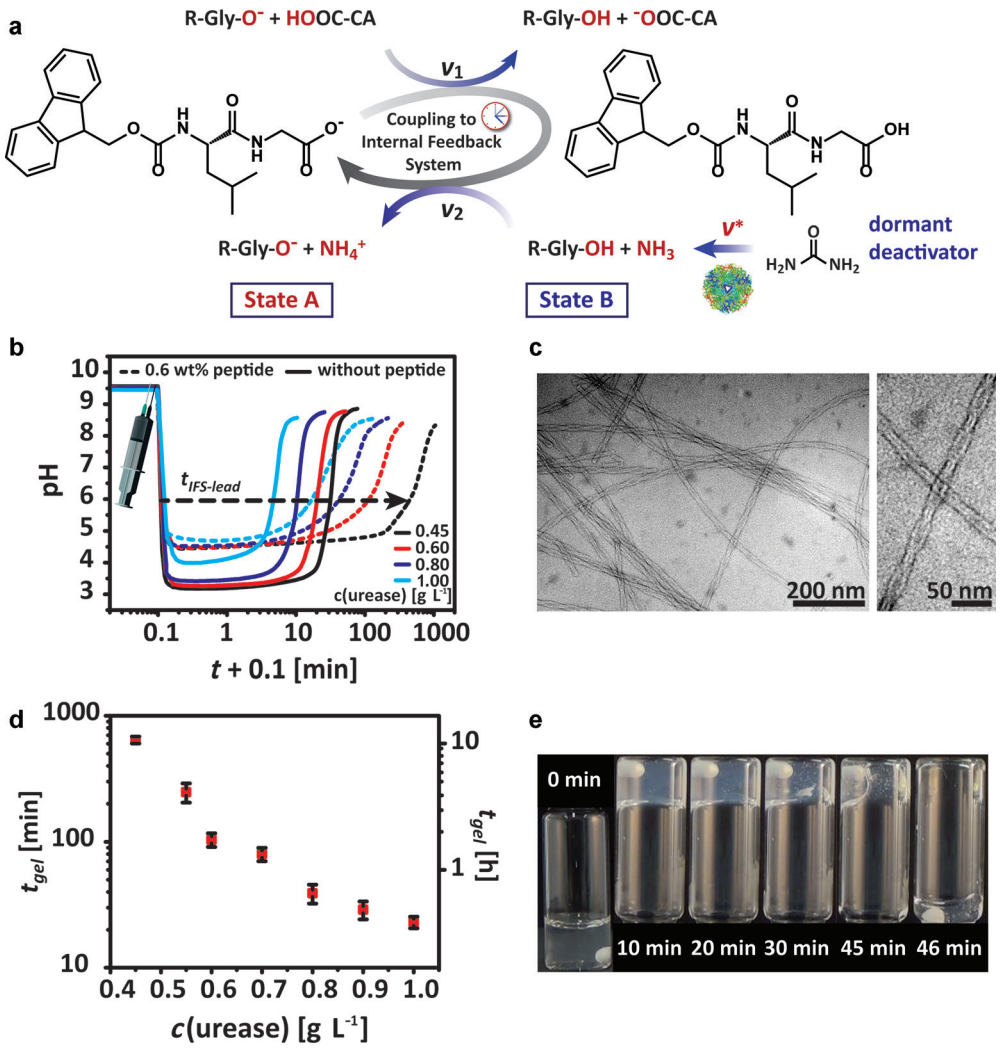

Figure 3. Temporal programing of Fmoc-Leu-Gly-OH dipeptide self-assemblies and hydrogels. a) Coupling of the dipeptide with the acidic IFS. b) Influence of the peptide on the pH–time profiles, as programmed by the use of different urease concentrations. c) Cryo-TEM images revealing the twisted structure of self-assembled nanofibrils. d) Gel lifetimes as determined by tube-inversion tests. e) Series of snapshots of a temporally programmed peptide hydrogel at a urease concentration of 0.8 g L^{-1}. Conditions for (b,d,e): 60 mM urea, 12 mM CA/Na_3C (9:1) buffer, and different urease concentrations as indicated.

behind the gel plug in the meantime, reactants could be diverted as needed, and fluid logic systems could be programmed.[21,22] Furthermore, self-erasing hydrogels open an avenue to burst-release systems and transient rapid prototyping. A comparison between a classical responsive micromolded hydrogel and a time-programmed self-erasing hydrogel is shown in Figure 4b (see also Movie S2). The classical gel will remain stable until an outside trigger is given, whereas the self-regulating hydrogel disappears on a time-programmed pathway, thus giving rise to a sudden and predictable burst release of encapsulated material (a dye in this case). The series of snapshots in Figure 4b again demonstrates the clear differences between passively responsive hydrogels and the self-regulating, dynamic hydrogels described herein.

In conclusion, we have demonstrated how to precisely program acidic pH profiles in time by the feedback-driven, biocatalytically controlled slow generation of a base in combination with fast acidic promoters in closed systems. We coupled such transient pH profiles to a responsive peptide gelator, thus enabling the programming of gel lifetimes. This approach can be viewed as an important advance with respect to classical stimuli-responsive materials, as it provides access to dynamic, self-regulating materials based on internal triggers. We also showed that time-programmed and self-erasing, injectable, and micromoldable hydrogels are useful for burst release or fluidic guidance. Since our approach modulates the surroundings of the material and does not chemically alter its structure beyond protonation, we believe it to be a simple and generic method that could be used to program the lifetimes of other self-assemblies that form at low pH values. It also promotes an understanding of challenging dynamic materials and systems. In future, advanced control over self-assembling systems with respect to time could be possible by the combination of dormant activators and deactivators, which would enable the definition of the "on time" before the self-assembly forms.

Acknowledgements

We acknowledge funding by the DFG under grant agreement WA3084/4-1. We thank A. Kühne for suggestions with regard to the microfluidic setup. This research was performed in part at the Center for Chemical Polymer Technology, supported by the EU and North Rhine-Westphalia (EFRE 30 00 883 02). A.W. acknowledges continuous support from M. Möller.

Keywords: dynamic materials · hydrogels · materials science · peptides · self-regulation

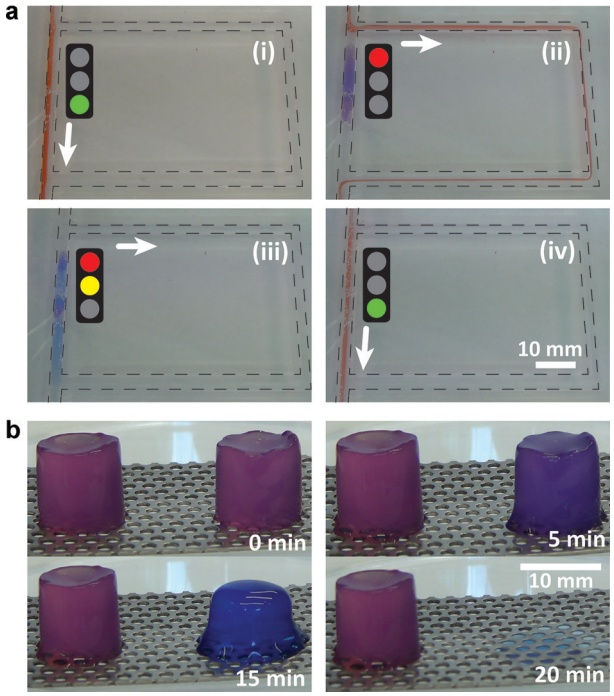

Figure 4. Fluidic guidance, burst release, and transient rapid prototyping by the use of time-programmed hydrogels. a) Fluidic guidance: i) The fluid prefers the direct pathway; ii) the bypass is used upon blocking of the dominant channel with the time-programmed hydrogel; iii, iv) upon dissolution of the hydrogel, the direction of the original fluid stream is recovered (1.3 $g\,L^{-1}$ urease, 60 mM urea, 12 mM CA/Na_3C (9:1) buffer, 1.5 wt% Fmoc-Leu-Gly, 150 μM resazurin, Congo red as an indicator dye for the fluid stream). b) Self-erasing hydrogels for burst release and transient rapid prototyping. Series of snapshots of two micromolded cylinders without (left) and with the IFS (right). Conditions: 1 wt% Fmoc-Leu-Gly, 1.3 $g\,L^{-1}$ urease, 12 mM CA/Na_3C (9:1) buffer, and (in the gel on the right) 60 mM urea.

How to cite: *Angew. Chem. Int. Ed.* **2015**, *54*, 13258–13262
Angew. Chem. **2015**, *127*, 13456–13460

[1] a) C. Stoffelen, J. Voskuhl, P. Jonkheijm, J. Huskens, *Angew. Chem. Int. Ed.* **2014**, *53*, 3400–3404; *Angew. Chem.* **2014**, *126*, 3468–3472; b) L. Chen, K. Morris, A. Laybourn, D. Elias, M. R. Hicks, A. Rodger, L. Serpell, D. J. Adams, *Langmuir* **2010**, *26*, 5232–5242.
[2] a) Y. Kang, J. J. Walish, T. Gorishnyy, E. L. Thomas, *Nat. Mater.* **2007**, *6*, 957–960; b) A. C. Arsenault, D. P. Puzzo, I. Manners, G. A. Ozin, *Nat. Photonics* **2007**, *1*, 468–472.
[3] M. Fidaleo, R. Lavecchia, *Chem. Biochem. Eng. Q.* **2003**, *17*, 311–318.
[4] a) C. T. Huynh, M. K. Nguyen, D. S. Lee, *Macromolecules* **2011**, *44*, 6629–6636; b) S. Yan, T. Wang, L. Feng, J. Zhu, K. Zhang, X. Chen, L. Cui, J. Yin, *Biomacromolecules* **2014**, *15*, 4495–4508; c) S. Zhang, M. A. Greenfield, A. Mata, L. C. Palmer, R. Bitton, J. R. Mantei, C. Aparicio, M. O. de La Cruz, S. I. Stupp, *Nat. Mater.* **2010**, *9*, 594–601; d) J.-F. Lutz, H. G. Börner, *Prog. Polym. Sci.* **2008**, *33*, 1–39.
[5] a) W. T. S. Huck, *Mater. Today* **2008**, *11*, 24–32; b) S. Moya, O. Azzaroni, T. Farhan, V. L. Osborne, W. T. S. Huck, *Angew. Chem. Int. Ed.* **2005**, *44*, 4578–4581; *Angew. Chem.* **2005**, *117*, 4654–4657.
[6] a) Y. Zhu, J. Shi, W. Shen, X. Dong, J. Feng, M. Ruan, Y. Li, *Angew. Chem. Int. Ed.* **2005**, *44*, 5083–5087; *Angew. Chem.* **2005**, *117*, 5213–5217; b) Y. Bae, S. Fukushima, A. Harada, K. Kataoka, *Angew. Chem. Int. Ed.* **2003**, *42*, 4640–4643; *Angew. Chem.* **2003**, *115*, 4788–4791.
[7] a) Y. Li, B. S. Lokitz, C. L. McCormick, *Angew. Chem. Int. Ed.* **2006**, *45*, 5792–5795; *Angew. Chem.* **2006**, *118*, 5924–5927; b) M. A. C. Stuart, W. T. S. Huck, J. Genzer, M. Müller, C. Ober, M. Stamm, G. B. Sukhorukov, I. Szleifer, V. V. Tsukruk, M. Urban, F. Winnik, S. Zauscher, I. Luzinov, S. Minko, *Nat. Mater.* **2010**, *9*, 101–113.
[8] a) D. A. Fletcher, R. D. Mullins, *Nature* **2010**, *463*, 485–492; b) T. Mitchison, M. Kirschner, *Nature* **1984**, *312*, 237–242; c) G. M. Whitesides, B. Grzybowski, *Science* **2002**, *295*, 2418–2421.
[9] a) C. Wang, R. J. Stewart, J. Kopecek, *Nature* **1999**, *397*, 417–420; b) A. M. Smith, R. J. Williams, C. Tang, P. Coppo, R. F. Collins, M. L. Turner, A. Saiani, R. V. Ulijn, *Adv. Mater.* **2008**, *20*, 37–41; c) A. Aggeli, M. Bell, N. Boden, L. M. Carrick, A. E. Strong, *Angew. Chem. Int. Ed.* **2003**, *42*, 5603–5606; *Angew. Chem.* **2003**, *115*, 5761–5764.
[10] a) S. Shinohara, T. Seki, T. Sakai, R. Yoshida, Y. Takeoka, *Angew. Chem. Int. Ed.* **2008**, *47*, 9039–9043; *Angew. Chem.* **2008**, *120*, 9179–9183; b) S. Maeda, Y. Hara, R. Yoshida, S. Hashimoto, *Angew. Chem. Int. Ed.* **2008**, *47*, 6690–6693; *Angew. Chem.* **2008**, *120*, 6792–6795; c) S. Maeda, Y. Hara, T. Sakai, R. Yoshida, S. Hashimoto, *Adv. Mater.* **2007**, *19*, 3480–3484.
[11] S. N. Semenov, A. S. Y. Wong, R. M. van der Made, S. G. J. Postma, J. Groen, H. W. H. van Roekel, T. F. A. de Greef, W. T. S. Huck, *Nat. Chem.* **2015**, *7*, 160–165.
[12] a) S. Debnath, S. Roy, R. V. Ulijn, *J. Am. Chem. Soc.* **2013**, *135*, 16789–16792; b) C. G. Pappas, I. R. Sasselli, R. V. Ulijn, *Angew. Chem. Int. Ed.* **2015**, *54*, 8119–8123; *Angew. Chem.* **2015**, *127*, 8237–8241.
[13] J. Boekhoven, A. M. Brizard, K. N. K. Kowlgi, G. J. M. Koper, R. Eelkema, J. H. van Esch, *Angew. Chem. Int. Ed.* **2010**, *49*, 4825–4828; *Angew. Chem.* **2010**, *122*, 4935–4938.
[14] T. Heuser, A.-K. Steppert, C. Molano Lopez, B. Zhu, A. Walther, *Nano Lett.* **2015**, *15*, 2213–2219.
[15] G. B. Kistiakowsky, A. J. Rosenberg, *J. Am. Chem. Soc.* **1952**, *74*, 5020–5025.
[16] A. J. Russell, M. Erbeldinger, J. J. DeFrank, J. Kaar, G. Drevon, *Biotechnol. Bioeng.* **2002**, *77*, 352–357.
[17] a) G. Hu, J. A. Pojman, S. K. Scott, M. M. Wrobel, A. F. Taylor, *J. Phys. Chem. B* **2010**, *114*, 14059–14063; b) J. M. Johnson, N. Kinsinger, C. Sun, D. Li, D. Kisailus, *J. Am. Chem. Soc.* **2012**, *134*, 13974–13977; c) R. de La Rica, H. Matsui, *Angew. Chem. Int. Ed.* **2008**, *47*, 5415–5417; *Angew. Chem.* **2008**, *120*, 5495–5497.
[18] T.-C. Huang, D.-H. Chen, *J. Chem. Technol. Biotechnol.* **1991**, *52*, 433–444.
[19] B. Krajewska, *J. Mol. Catal. B* **2009**, *59*, 9–21.
[20] C. Tang, R. V. Ulijn, A. Saiani, *Langmuir* **2011**, *27*, 14438–14449.
[21] a) A. J. deMello, *Nature* **2006**, *442*, 394–402; b) M. Prakash, N. Gershenfeld, *Science* **2007**, *315*, 832–835.
[22] A. Lenshof, T. Laurell, *Chem. Soc. Rev.* **2010**, *39*, 1203–1217.

Received: June 2, 2015
Published online: August 6, 2015